



HAL
open science

Apathy in depression: An arterial spin labeling perfusion MRI study

Jean-Marie Batail, Isabelle Corouge, Benoit Combès, Camille Conan, Muriel Guillery-Sollier, Marc Vérin, Paul Sauleau, Florence Le Jeune, Jean-Yves Gauvrit, Jen-Yves Gauvrit, et al.

► **To cite this version:**

Jean-Marie Batail, Isabelle Corouge, Benoit Combès, Camille Conan, Muriel Guillery-Sollier, et al.. Apathy in depression: An arterial spin labeling perfusion MRI study. *Journal of Psychiatric Research*, 2023, 157, pp.7-16. 10.1016/j.jpsychires.2022.11.015 . inserm-03866929

HAL Id: inserm-03866929

<https://inserm.hal.science/inserm-03866929>

Submitted on 1 Sep 2023

HAL is a multi-disciplinary open access archive for the deposit and dissemination of scientific research documents, whether they are published or not. The documents may come from teaching and research institutions in France or abroad, or from public or private research centers.

L'archive ouverte pluridisciplinaire **HAL**, est destinée au dépôt et à la diffusion de documents scientifiques de niveau recherche, publiés ou non, émanant des établissements d'enseignement et de recherche français ou étrangers, des laboratoires publics ou privés.



Distributed under a Creative Commons Attribution 4.0 International License



Apathy in depression: An arterial spin labeling perfusion MRI study

J.M. Batail^{a,b,c,*}, I. Corouge^{b,1}, B. Combès^b, C. Conan^a, M. Guillery-Sollier^{a,c,d}, M. Vérin^{c,e},
P. Sauleau^{c,f}, F. Le Jeune^{c,g}, J.Y. Gauvrit^{b,h}, G. Robert^{a,b,c}, C. Barillot^b, J.C. Ferre^{b,h},
D. Drapier^{a,c}

^a Centre Hospitalier Guillaume Régnier, Pôle Hospitalo-Universitaire de Psychiatrie Adulte, F-35703, Rennes, France

^b Univ Rennes, Inria, CNRS, IRISA, INSERM, Empenn U1228 ERL, F-35042, Rennes, France

^c Univ Rennes, “Comportement et noyaux gris centraux” Research Unit (EA 4712), F-35000, Rennes, France

^d Univ Rennes, LP3C (Laboratoire de Psychologie: Cognition, Comportement, Communication) - EA 1285, CC5000, Rennes, France

^e CHU Rennes, Department of Neurology, F-35033, Rennes, France

^f CHU Rennes, Department of Neurophysiology, F-35033, Rennes, France

^g Centre Eugène Marquis, Department of Nuclear Medicine, F-35062, Rennes, France

^h CHU Rennes, Department of Radiology, F-35033, Rennes, France

ARTICLE INFO

Keywords:

Depressive disorder
Arterial spin labeling
Perfusion MRI
Apathy
Neuroimaging

ABSTRACT

Introduction: Apathy, as defined as a deficit in goal-directed behaviors, is a critical clinical dimension in depression associated with chronic impairment. Little is known about its cerebral perfusion specificities in depression. To explore neurovascular mechanisms underpinning apathy in depression by pseudo-continuous arterial spin labeling (pCASL) magnetic resonance imaging (MRI).

Methods: Perfusion imaging analysis was performed on 90 depressed patients included in a prospective study between November 2014 and February 2017. Imaging data included anatomical 3D T1-weighted and perfusion pCASL sequences. A multiple regression analysis relating the quantified cerebral blood flow (CBF) in different regions of interest defined from the FreeSurfer atlas, to the Apathy Evaluation Scale (AES) total score was conducted.

Results: After confound adjustment (demographics, disease and clinical characteristics) and correction for multiple comparisons, we observed a strong negative relationship between the CBF in the left anterior cingulate cortex (ACC) and the AES score (standardized beta = -0.74 , corrected p value = 0.0008).

Conclusion: Our results emphasized the left ACC as a key region involved in apathy severity in a population of depressed participants. Perfusion correlates of apathy in depression evidenced in this study may contribute to characterize different phenotypes of depression.

1. Introduction

Apathy is now well recognized as an important behavioral syndrome in several neuropsychiatric disorders (Marin, 1990; 1991; 1996). It is widely agreed that apathy is a transnosographic syndrome, found in various neurological disorders, such as Alzheimer's Disease (AD), Parkinson's Disease (PD) and other dementias, traumatic brain injury and stroke, but also in psychiatric disorders including schizophrenia and major depressive disorder (van Reekum et al., 2005). Apathy has a dramatic clinical and prognostic impact marked by impairment of activities of daily living (Freels et al., 1992), cognitive impairment with

executive dysfunction (Zahodne and Tremont, 2013), increased risk of conversion to dementia (Vicini Chilovi et al., 2009), decreased response to treatment (Kos et al., 2016) and diminished quality of life (Prakash et al., 2016).

Apathy has been extensively studied in neurodegenerative disorders using several imaging modalities assessing either cerebral metabolism or brain perfusion or with different image analyses such as morphometry or functional connectivity. Regarding apathy in Parkinson's disease (PD), neuroimaging positron emission tomography (PET) studies are contradictory, demonstrating either a negative correlation between apathy and cerebral metabolism in the striatum, cerebellum, and prefrontal,

* Corresponding author. Centre Hospitalier Guillaume Régnier, 108 avenue du Général Leclerc, 35703, Rennes, France.

E-mail address: jeanmariebatail@gmail.com (J.M. Batail).

¹ These authors contributed equally to this work.

<https://doi.org/10.1016/j.jpsychires.2022.11.015>

Received 8 December 2021; Received in revised form 28 July 2022; Accepted 12 November 2022

Available online 17 November 2022

0022-3956/© 2022 Published by Elsevier Ltd.

temporal, parietal and limbic lobes or a positive correlation between apathy and prefrontal, temporal, parietal and limbic areas (Robert et al., 2012, 2014; Wen et al., 2016). Functional magnetic resonance imaging (fMRI) showed a decreased connectivity between the left striatal and frontal areas (Baggio et al., 2015) while T1 weighted imaging reported increased atrophy in the frontal and parietal lobes, insula and left nucleus accumbens in apathetic patients (Wen et al., 2016). In Alzheimer's disease, most studies linked apathy with the anterior cingulate cortex (ACC), the medial frontal cortex and some of them also involved the orbitofrontal cortex (Theleritis et al., 2014). A recent review conceptualized the biological basis of motivation based behaviors as a coordination of three systems: (a) a "valuation system", composed by the ventromedial prefrontal cortex and the ventral striatum, involved in cost-effort/benefit balance evaluation of the stimuli, (b) a "mediating system", composed of the anterior cingulate cortex and the caudate, that uses this information to trigger a motor action towards a particular goal that is performed by (c) a "motor system" composed by the supplementary motor area (SMA), the posterior cingulate cortex (PCC) and the dorsal putamen (Le Heron et al., 2019). So, apathy affects a large meso-cortico-limbic circuit (Benoit and Robert, 2011; Kos et al., 2016; Kostić and Filippi, 2011; Le Heron et al., 2019; Theleritis et al., 2014; Wen et al., 2016).

Apathy has also been investigated in late-life depression and some studies have identified the involvement of accumbens and ACC, structures belonging to reward processing (Alexopoulos et al., 2012; Yuen et al., 2014a,b). Few studies have addressed the neuroanatomical correlates of apathy in adult depression. First, a study reported that apathetic depressed patients, although they had a motivation deficit, had preserved self-reported capacity to feel pleasure compared to non-aphathetic ones (Batail et al., 2018). These findings suggested the existence of different biological profiles of depression depending on the intensity of comorbid apathy, in terms of motivational dimension and sensitivity to reward. In a recent work, Robert et al. reported, in a population of depressed women, that higher levels of apathy were associated with greater connectivity between dorsolateral prefrontal cortex (DLPFC) and ACC during an fMRI task with a high attentional load (Robert et al., 2021). They discussed this result as a functional response to restore pathological imbalance related to a deficit of motivation (Hillary et al., 2015). To date, no study has explored cerebral perfusion specificities of apathy in depression which could bring another level of understanding of its neurobiological mechanism. Indeed, apathy appears to be a good candidate for the identification of relevant biomarkers to guide antidepressant therapeutics. Following the call for a stratified psychiatry to move from a "one-size-fits-all psychiatry to more personalized-psychiatry" approach, there is a need to improve our understanding of which critical depression subtypes from both clinical and biological perspectives (Arns et al., 2022) could be of interest to explore. As an illustration, a recent study has demonstrated that current clinical classifications of depression subtypes were of limited usefulness in terms of prediction of antidepressant responsiveness and therefore for guidance in terms of AD choice (Arnou et al., 2015). Our work aims to bring some evidence in the consideration of apathy, and its biological substrates, as a relevant biomarker.

In particular, Arterial Spin Labeling (ASL) is a growing technique for perfusion brain imaging. This method is non-invasive and allows an absolute quantification of cerebral blood flow (CBF) (Detre et al., 1992). Given these advantages, ASL has been described as a reliable alternative to nuclear medicine-based perfusion imaging techniques. Furthermore, ASL allows an accurate perfusion analysis and can be considered as a proxy for cerebral metabolic and synaptic function which is of high interest in studying pathophysiological patterns in neuropsychiatric disorders such as depression (Watts et al., 2013). Thus, it has shown a good correlation between measured perfusion abnormalities and microcirculatory deficits and clinical symptoms (Théberge, 2008). In addition, test-retest studies highlighted a reasonable reproducibility (Ferré et al., 2013; Petersen et al., 2010). Altogether, because of its sensitivity and

discriminant power in specific disorders (Wolf and Detre, 2007), ASL is a modality which is suggested as a relevant tool to explore biomarkers of pathological brain functions (Detre et al., 2012) and particularly in depression (Watts et al., 2013).

However, only few works have used the ASL technique to study depression as in adolescents (Ho et al., 2013), adults (Orosz et al., 2012), treatment resistance (Duhameau et al., 2010; Lui et al., 2009), or late-life depression (Colloby et al., 2012). As pointed out previously, ASL could be a useful marker for identifying specific patterns of CBF abnormalities associated with different subtypes of depression (Haller et al., 2016). To date, only one study has investigated CBF (using ⁹⁹Tc-HMPAO single photon emission computed tomography) in a population of AD suffering from either depression or apathy. The authors have suggested that apathy and depression in AD involve distinct functional circuits (Kang et al., 2012). But no perfusion imaging study has yet investigated apathy in depression without neurodegenerative disorder.

The aim of this study was to assess the perfusion characteristics of apathy in depression by arterial spin labeling MRI. We hypothesized that cerebral perfusion, as measured by ASL, in key regions involved in emotional or reward processing are associated with apathy.

2. Methods

2.1. Participants

A prospective study was conducted. It was approved by a national ethic committee and registered at www.clinicaltrials.gov (NCT02286024). A complete description of the study was given to the subjects and their written informed consent was obtained. All patients were recruited between November 2014 and February 2017 from the adult psychiatry department of Rennes, France.

The study was proposed to patients suffering from a Mood Depressive Episode (MDE) under DSM IV criterion with or without personal history of Mood Depressive Disorder (unipolar or bipolar subtype). Exclusion criteria included other Axis I disorder (except anxious comorbidities such as post-traumatic stress disorder, social phobia, generalized anxiety disorder, panic disorder) which were explored using the Mini-International Neuropsychiatric Interview (M.I.N.I.) (Sheehan et al., 1998). Patients with severe chronic physical illnesses were not included. Other exclusion criteria were potential safety contraindications for MRI (pacemakers, metal implants, pregnancy and lactation), neurological problems or a history of significant head injury and significant circulatory conditions that could affect cerebral circulation (i.e., non-controlled hypertension). All patients underwent a neurological examination by a trained physician to ensure that no included subject had any clinical sign of dementia or abnormal neurological examination.

After clinical assessment, patients underwent an imaging protocol by a maximum of three days. Out of the 124 screened patients, 4 had to be excluded for clinical reasons, 8 for withdrawal of participation prior to the MRI evaluation, 2 for missing clinical data and 20 for radiological reasons (1 because of a frontal cyst and 19 because of dental material that caused large artifacts in the perfusion images) which results in a population sample of 90 patients (Fig. 1). The image data were anonymously stored into Shanoir, a dedicated environment to manage brain imaging research repositories (Barillot et al., 2016).

2.2. Clinical assessment

Patients were assessed by a single structured clinical interview led by a trained psychiatrist with the following scales:

- Mini-International Neuropsychiatric Interview (M.I.N.I.) (Sheehan et al., 1998)
- Apathy Evaluation Scale (AES) (Marin, 1991)
- Widlöcher Depressive Retardation Scale (WDRS) (Widlöcher, 1983)

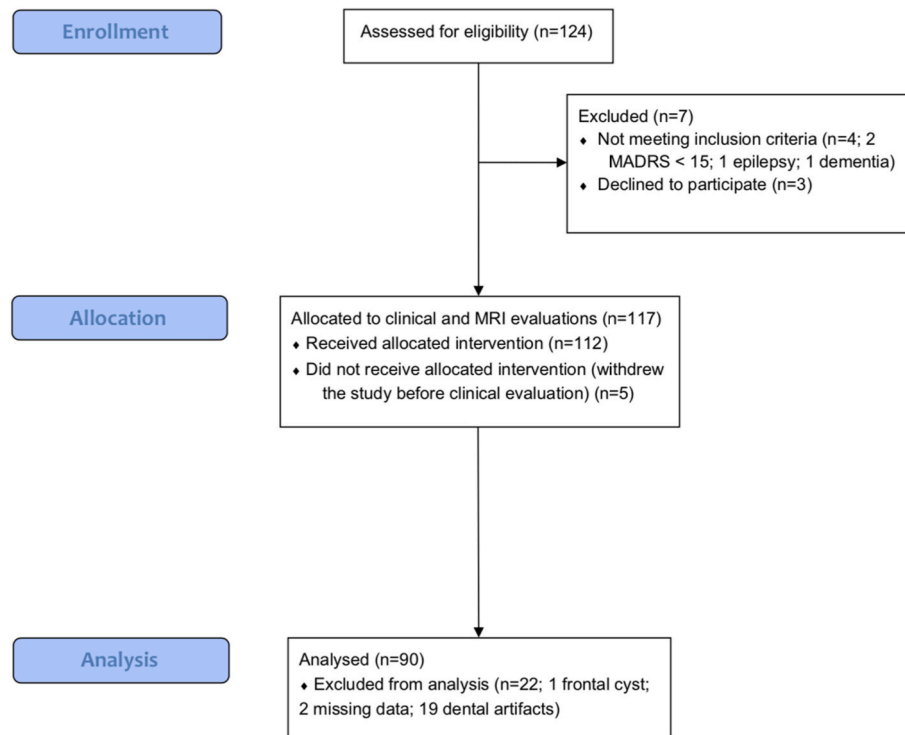


Fig. 1. Recruitment process.

- Montgomery and Åsberg Depression Rating Scale (MADRS) (Montgomery and Åsberg, 1979)
- State Trait Anxiety Inventory (STAI) (Spielberger et al., 1970)
- Snaith Hamilton Pleasure Scale (SHAPS) (Snaith et al., 1995)

Socio-demographic (age, gender) and disease characteristics (duration of disease, duration of episode, number of previous mood depressive episodes, medication status) were collected. Medication status of each patient was defined as the medication load score described by Almeida and colleagues (Almeida et al., 2009). This is a composite score reflecting both the dose and the variety of treatment (antidepressant, mood stabilizer, antipsychotic, anxiolytic). It is obtained by summing all individual medication scores for each medication category for each patient.

Table 1 describes our sample and Fig. 2 illustrates the pairwise correlations between all these variables.

The whole sample was characterized by a moderate depression intensity with middle-aged patients, predominantly women. Overall, looking at the pairwise correlations, the demographics, disease and clinical variables correlate weakly to moderately, all coefficients being below 0.4 (except for correlation between duration of disease and number of previous MDE; Spearman $\rho = 0.64$) (Fig. 2). When focusing on AES, the most pronounced correlations were observed for the psychomotor retardation score (WDRS, $\rho = -0.25$) and the anhedonia score (SHAPS, $\rho = -0.21$) (Table 1).

2.3. MRI data acquisition

Patients were scanned on a 3T whole body Siemens MR scanner (Magnetom Verio, Siemens Healthcare, Erlangen, Germany) with a 32-channel head coil. Anatomical data included a high-resolution 3D T1-weighted MPRAGE sequence (3D T1w) with the following imaging parameters: TR/TE/TI = 1900/2.26/900 ms, $256 \times 256 \text{ mm}^2$ FOV and 176 sagittal slices, $1 \times 1 \text{ mm}^3$ resolution, parallel imaging with GRAPPA factor 2. Perfusion data were acquired using a pseudo-continuous ASL sequence with a total scan time of approximately 4 min (Wu et al.,

Table 1

Population description (whole sample; n = 90): Descriptive statistics for the demographics, disease and clinical characteristics are given for the whole sample in the middle column. The Spearman correlation coefficients between the AES score and the other variables are given in the right column along with the confidence intervals at 95%. MAD stands for median absolute deviation.

Variable n = 90	Whole sample (n = 90) Median [range] \pm MAD or n (%)	Spearman correlation coefficient (ρ) with confidence intervals at 95%
AES	38.5 [24; 59] \pm 4.5	–
Age	49.5 [18; 74] \pm 10.5	0.02 [-0.19; 0.23]
Gender (female)	60 (66.67%)	–
Current MDE duration (weeks)	13 [0; 150] \pm 9	-0.14 [-0.34; 0.07]
Duration of disease (years)	12 [0; 57] \pm 8	0.04 [-0.17; 0.25]
Number of previous MDE	3 [0; 30] \pm 1	0.13 [-0.08; 0.33]
Medication load	3 [1; 7] \pm 1	-0.04 [-0.24; 0.17]
MADRS (total score)	27 [16; 42] \pm 3.5	-0.10 [-0.30; 0.11]
WDRS (total score)	22 [2; 43] \pm 7	-0.25 [-0.43; -0.04]
STAI YA (total score)	58 [28; 80] \pm 9	-0.10 [-0.30; 0.11]
STAI YB (total score)	59.5 [30; 79] \pm 8	0.02 [-0.19; 0.22]
SHAPS (total score)	5 [0; 14] \pm 3	-0.21 [-0.40; 0.00]

2007). The imaging parameters were: TR/TE = 4000/12 ms, flip angle 90° , matrix size 64×64 , labeling duration (LD)/post-labeling delay (PLD) = 1500/1500 ms, parallel imaging SENSE factor 2. The labeling plane was placed 9 cm below the center of the acquisition volume. Twenty axial slices were acquired sequentially from inferior to superior in the AC-PC plane, with $3.5 \times 3.5 \text{ mm}^2$ in-plane resolution, 5 mm slice thickness and 1 mm gap. Thirty repetitions, i.e., label/control pairs, finally composed the ASL data series (overall 60 vol). Additionally, M0 images were acquired at the same dimension and resolution as

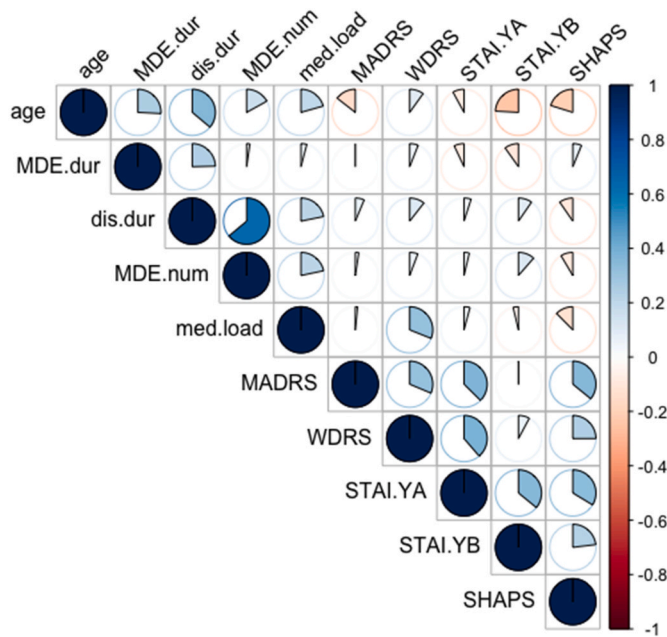


Fig. 2. Demographics, disease and clinical variables: visual representation of pairwise Spearman correlations. The areas of circles show the absolute value of corresponding correlation coefficients, the blue color encodes positive correlation while the red color encodes negative correlation. The more the circle is filled and the stronger the color is, the higher is the correlation coefficient. “MDE.dur” stands for the actual MDE duration, “dis.dur” for duration of disease, “MDE.num” for number of previous MDE and “med.load” for medication load. For example, the circle between dis.dur and MDE.num represents a positive correlation of 0.6 whereas no correlation has been found between med.load and MADRS (circle almost empty).

equilibrium magnetization maps (TR/TE = 10/12 s).

2.4. MRI data processing

Processing of the image data was performed with our AutoMRI² in-house pipeline using MATLAB (v. R2014a, The MathWorks Inc.) and the SPM8 toolbox (Wellcome Department of Imaging Neuroscience at University College London, UK). An overview of our data pre-processing is illustrated in Fig. 3.

The anatomical 3D T1w was corrected for intensity inhomogeneity and segmented into grey matter (GM), white matter (WM) and cerebrospinal fluid (CSF) probability maps using the MNI ICBM152 template tissue probability as an a priori for brain tissue classification. This was done using the unified segmentation model SPM routine, which also estimates the spatial normalization parameters (Ashburner and Friston, 2005). The latter were applied to warp the 3D T1w volume to the MNI template.

The ASL data series was motion corrected by a rigid body transformation minimizing the sum of squared differences cost function. A two-pass procedure first realigned all the control and label volumes onto the first volume of the series, then registered the series to the mean of the images aligned in the first pass. The motion-corrected ASL series was co-registered to the 3D T1w using a rigid transformation. The latter was estimated by maximizing normalized mutual information between the mean control images, i.e., the average of all the realigned control volumes, and the 3D T1w GM map. The co-registered ASL images were then pairwise subtracted (control - label images) to produce a series of perfusion-weighted maps, which could be subsequently averaged by arithmetic sample mean to produce a perfusion weighted (PW) map.

However, as the sample mean is very sensitive to outliers, we instead use Huber’s M-estimator to robustly estimate the PW map (Maumet et al., 2014). This robust PW map was eventually quantified to a CBF map by applying the standard kinetic model (Buxton et al., 1998):

$$f = 6000 \cdot \frac{\lambda \Delta M e^{\frac{PLD + idx_{sl} + T_{1b}}{T_{1b}}}}{2\alpha T_{1b} (1 - e^{\frac{-t}{T_{1b}}}) M_0} \text{ [ml/100g/min]}$$

where f is the CBF map, ΔM is the perfusion weighted map, $\lambda = 0.9 \text{ ml g}^{-1}$ is the blood/tissue water partition coefficient, $\alpha = 0.85$ measures the labeling efficiency, $T_{1b} = 1650 \text{ ms}$ is the T_1 of blood (Alsop et al., 2015), M_0 represents the equilibrium magnetization of arterial blood, $PLD = 1500 \text{ ms}$ is the post-labeling delay of the ASL sequence, $\tau = 1500 \text{ ms}$ is the labeling duration, idx_{sl} is the slice index, starting from 0 for the first acquired slice, $TI_{sl} = 37 \text{ ms}$ is the acquisition duration of one slice.

For subsequent region of interest (ROI) analysis, a set of anatomical ROIs was delineated for each patient. The ROIs were selected in reference to theoretical foundational works in the field of biology of goal directed behaviors (Berridge et al., 2009; Le Heron et al., 2019). These works emphasize that such behaviors depend on three systems involved in the valuation, mediation of reward sensitivity and motor aspect of goal-directed behavior. Also, these theories refer to the concepts of “liking” or consummatory anhedonia and “wanting” or motivational anhedonia (Berridge et al., 2009; Gaillard et al., 2013). Based on this anatomical and functional hypothesis, we a priori selected our ROIs, to explore these systems and address our scientific question. The ROIs were extracted from the Desikan-Killiany Atlas (Desikan et al., 2006) using the FreeSurfer software³ and were selected in light of the literature about apathy and neuroimaging (Berridge et al., 2009; Gaillard et al., 2013; Kang et al., 2012; Treadway and Zald, 2011). They were: thalamus, caudate, putamen, pallidum, amygdala, insula, accumbens nucleus, PCC, anterior cingulate cortex, orbitofrontal cortex (OFC), frontal cortex (superior, middle and inferior parts) for the left and right hemispheres, that is 26 areas in total. The anterior cingulate cortex was defined as the union of the FreeSurfer ROIs “ctx-caudalanteriorcingulate” and “ctx-rostralanteriorcingulate”, the orbitofrontal cortex as the union of “ctx-lateralorbitofrontal” and “ctx-medialorbitofrontal” and the middle frontal cortex as the union of “ctx-caudalmiddlefrontal” and “ctx-rostralmiddlefrontal”, the inferior frontal cortex as the union of “ctx-parsopercularis” and “ctx-parsorbitalis” and “parstriangularis”.

Last, the mean CBF values were computed for each subject over each ROI in the MNI space. To discard outliers that may be present in particular at GM/LCS interface due to the low resolution of ASL, we used the modified z-score proposed by Iglewicz and Hoaglin (Iglewicz and Hoaglin, 1993) before computing the average CBF value in a given ROI:

$$Z_i = \frac{0.6745(x_i - \tilde{x})}{MAD}$$

where \tilde{x} denotes the median over the ROI and MAD the median absolute deviation.⁴ Voxels x_i with a Z_i score greater than 3.5 were discarded.

In addition, to account for global CBF level differences across participants in subsequent statistical analysis, the CBF values were scaled by the average CBF over grey matter, i.e., for each patient and each ROI, normalized CBF values were computed as the fraction “mean CBF value over the ROI/mean CBF over patient GM”. Henceforth, we will only consider these normalized CBF values.

2.5. Perfusion MRI data statistical analysis

The statistical analysis was performed on the 90 patients included in this perfusion study (intention-to-treat analysis) with R software

³ <http://surfer.nmr.mgh.harvard.edu/fswiki/>.

⁴ The median absolute deviation is defined as $MAD = \text{median}(x_i - \tilde{x})$ where x denotes the median of the data and x the absolute value of x .

² <https://team.inria.fr/visages/software/>.

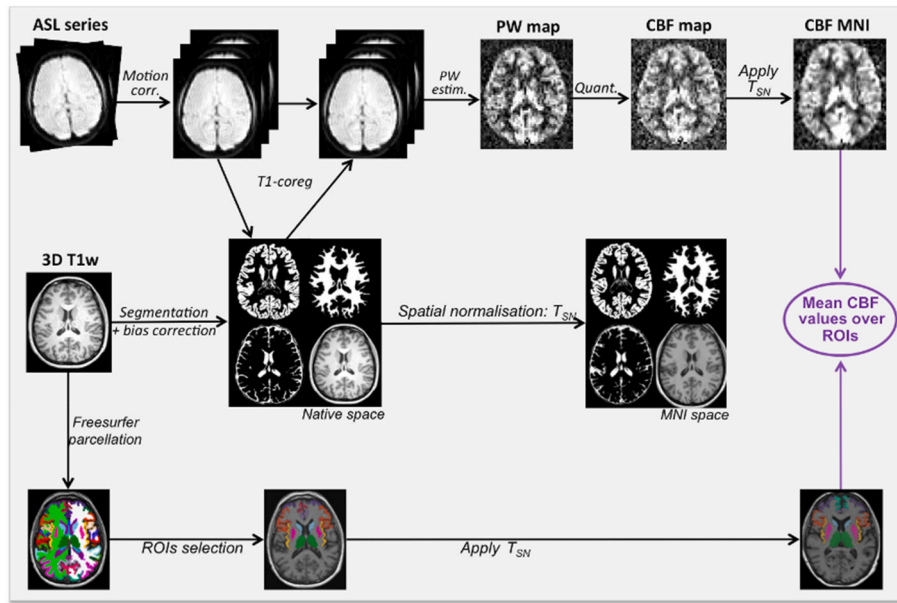


Fig. 3. Overview of our data pre-processing pipeline.

(<http://www.R-project.org/>).

2.6. ROI-based description of perfusion

As explained in section 2.4, the normalized CBF values were computed from the ASL data for each subject and averaged over each ROI.

In order to explore the spatial perfusion patterns between the anatomical ROIs and to visualize the relationships between their respective CBFs, we compute the dendrogram of the Spearman correlations (function *varclus* from R-Hmisc package⁵). This intended to give a comprehensive description of our ROIs brain perfusion data set at the group level and how ROIs correlated to each other. The dendrogram is a “tree-like” diagram built by hierarchical clustering using in this case, the Spearman coefficient as the similarity measure. At the leaf level, it can be seen as a summary of the ROI-CBFs correlation matrix.

2.6.1. Explanatory ASL modeling of apathy

To assess the perfusion correlates of apathy in depression, we investigated the effect of CBF patterns in the different ROIs on the associated apathy score.

For this purpose, we performed a stepwise variable selection on a linear model with apathy, i.e., the AES score, as the dependent variable. We included as linear predictor candidates (or intersect, for categorical variables) the normalized CBF values in the 26 different ROIs, the mean CBF value over the grey matter as well as the patients demographic variables (age, gender) and disease and clinical characteristics (actual MDE duration, duration of disease, number of previous MDE, medication load, MADRS total score, WDRS total score, SHAPS total score, STAI YA and STAI YB total scores). Akaike’s information criterion was used as the inclusion and rejection rule. Then, for each independent variable in the resulting reduced model, the associated standardized beta coefficients along with their 95% confidence intervals and p-values associated to “beta coefficient = 0” were computed. Moreover, we also reported p-values adjusted for multiple comparisons using a Bonferroni correction accounting for the overall number of initial parameters of interest (38 in our case). Effects associated with p-values lower than 0.05 after this Bonferroni correction were considered as significant.

3. Results

3.1. ROI-based description of perfusion

The raw and normalized CBF values in the 26 ROIs as well as their pairwise correlations are presented in supplementary material.

The dendrogram in Fig. 4 shows that most of the time, the highest correlated area for a given ROI is its contralateral part. This is for instance the case for ACC left and right ($\rho = 0.65$) and for OFC left and right ($\rho = 0.65$ also).

3.2. Explanatory ASL modeling of apathy

Table 2 summarizes the linear fitting of apathy, i.e., the AES score, by the ROI-CBFs variables while accounting for demographic, disease and clinical variables.

This table lists the regressors corresponding to the selected variables from the stepwise regression and presents their standardized beta estimates along with their associated 95% confidence intervals as well as both uncorrected and Bonferroni corrected p-values.

To assess the reliability of our analysis, we visually checked residuals and Q-Q plots, scale-location plots and residual versus leverage plots. Moreover, to assess the reliability of our multivariate regression model, we visually checked residuals and Q-Q plots, scale-location, residual versus leverage and series residuals plots. Moreover, the absence of strong collinearity between independent variables was checked using variance inflation factors. These additional analyses are in Figs. 3 and 4 of supplemental material.

From Table 2, we observe evidence of:

- a negative regression slope for left anterior cingulate cortex, left orbito-frontal cortex (OFC), right putamen, left thalamus, right inferior frontal gyrus (IFG)
- a positive regression slope for left caudate nucleus, right anterior cingulate cortex, right insula, left medial frontal gyrus, left accumbens nucleus.

Moreover, after correction for multiple comparisons, the left ACC CBF remains significant with standardized beta = -0.74 , ($[-1.07, -0.42]$) and corrected p-value < 0.001 (Table 2 and Fig. 5).

⁵ <https://rdrr.io/cran/Hmisc/man/varclus.html>.

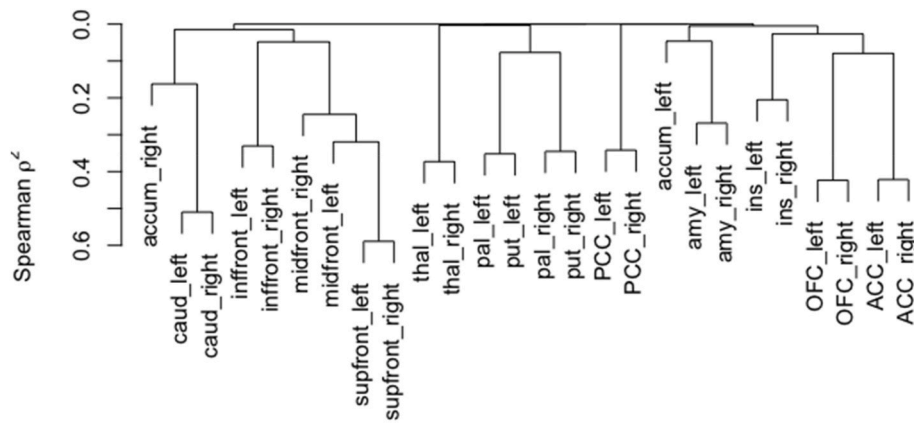


Fig. 4. Dendrogram of the Spearman correlations coefficients between the normalized CBFs of the 26 ROIs. accum: accumbens nucleus; amy: amygdala; caud: caudate nucleus; inffront: inferior frontal gyrus; ins: insula; midfront: middle frontal gyrus; pal: pallidum; put: putamen; supfront: superior frontal gyrus; thal: thalamus.

Table 2

ROI-CBFs, demographics, disease and clinical variables effects on apathy (AES score) from a linear regression using a stepwise variable selection. The left column lists the selected variables, the second column gives their standardized beta estimates along with their associated 95% confidence intervals while the third and fourth columns show associated uncorrected and Bonferroni corrected p-values for “standardized beta = 0”. ACC: anterior cingulate cortex; accum: accumbens nucleus; caud: caudate nucleus; inffront: inferior frontal gyrus; ins: insula; mean_gm: mean grey matter cerebral blood flow; MDE.dur: duration of current depressive episode; MDE.num: number of previous MDE; midfront: middle frontal gyrus; OFC: orbito-frontal cortex; pal: pallidum; put: putamen; thal: thalamus; WDRS: Widlöcher depressive retardation scale.

ROI	standardized beta with confidence intervals at 95%	p-value for standardized beta = 0	adjusted p-value (Bonferroni correction)
ACC_left	-0.74 [-1.07; -0.42]	<0.0001	0.0008
ACC_right	0.38 [0.08; 0.68]	0.013	0.51
caud_left	0.36 [0.10; 0.63]	0.008	0.29
ins_right	0.35 [0.07; 0.63]	0.014	0.55
put_right	-0.31 [-0.61; -0.02]	0.037	1
midfront_left	0.30 [0.06; 0.55]	0.017	0.65
put_left	0.28 [-0.02; 0.58]	0.069	1
WDRS	-0.27 [-0.47; -0.08]	0.007	0.26
OFC_left	-0.27 [-0.48; -0.05]	0.014	0.55
age	0.23 [0.002; 0.45]	0.048	1
inffront_right	-0.22 [-0.47; 0.03]	0.082	1
mean_gm	0.21 [-0.01; 0.44]	0.066	1
thal_left	-0.20 [-0.43; 0.02]	0.078	1
MDE.dur	-0.16 [-0.35; 0.03]	0.088	1
accum_left	0.15 [-0.04; 0.35]	0.127	1
MDE.num	0.13 [-0.05; 0.32]	0.158	1

4. Discussion

Our results from 90 depressed participants evidenced significant associations between apathy intensity and ASL perfusion in some regions, once accounting for confounding variables (age, gender, number of MDE, MDE duration, mean grey matter CBF and psychomotor retardation).

After adjustment for multiple comparisons, the most robust result was a strong negative relationship between CBF in the left ACC and the AES score (standardized beta = -0.74, corrected p value = 0.0008).

4.1. Role of anterior cingulate cortex

The ACC is located in the medial portion of each hemisphere, in direct connection to both limbic “emotional” and prefrontal “cognitive” systems. This large region is composed of Brodmann areas (BA) 24, 25,

32, 33, with functionally division between the caudal sub-regions (caudal portion of BA 24, and BA 32, 33) involved in cognition and the rostral sub-regions (rostral portion of BA 24, and BA 25) involved in emotion regulation. This region is known to have a key role in driving mechanisms that associate affect and cognition (Devinsky et al., 1995). More precisely, the ACC has been identified to mediate the cognitive influences on emotions (Stevens et al., 2011).

ACC is thought to have a role in emotionally driven behaviors. Indeed, reduced activity of the cingulate cortex, secondary to lesions, such as stroke, epilepsy, psychosurgery, have been associated with diminished self-awareness, akinetic mutism, depression, impaired motor initiation (Devinsky et al., 1995). Recent works have reported a high-level integrative role of the ACC in the regulation of behaviors in the context of goal directed action (Holroyd and Yeung, 2012) or socially driven interactions (Lavin et al., 2013). This key region is described to have multiple roles such as affective evaluation in contexts that demand adaptation (Braem et al., 2017), exploration of alternatives - crucial in decision making - adaptation of action (Brockett et al., 2020) and maintenance of goal-directed behaviors (Kolling et al., 2016).

Taken together, ACC seems to have a role of integration of emotional salience of stimuli, cognitive control and behavioral response to situations that potentially need effort (Gasquoine, 2013; Le Heron et al., 2019). Our study identified this brain area as a key structure that is associated with apathy intensity in depressed patients. We have to notice that the effect size reported highlights the central role of this region in apathy in depression. This result is of interest because it brings another proof of ACC’s involvement in a neuropsychiatric disease - such as depression - which is characterized by emotion dysregulation and cognitive control deficit (Chen et al., 2013; Etkin et al., 2015). More precisely, given this literature and our results, ACC perfusion could be considered as a surrogate of goal-directed behaviors in depression.

4.2. Goal-directed behaviors and anterior cingulate cortex

Following this assumption, ACC has been shown with a critical role in selecting and maintaining behaviors related to reward sensitivity, central in goal-directed behaviors (Holroyd and Yeung, 2012). More precisely his role is thought to be central in the transformation of effort into goal-directed behavior (Bonnelle et al., 2016; Holroyd and McClure, 2015; for review: Le Heron et al., 2019).

In a study by Onoda and Yamaguchi, a graph theory analysis has emphasized abnormalities of nodal efficiency linked with apathy (Onoda and Yamaguchi, 2015). Nodal efficiency is defined as the ability of information propagation between a given node with the rest of the nodes in a network. Higher nodal efficiency is indicative of higher integration in the brain. In this study, decreased nodal efficiency in ACC was a significant predictor of

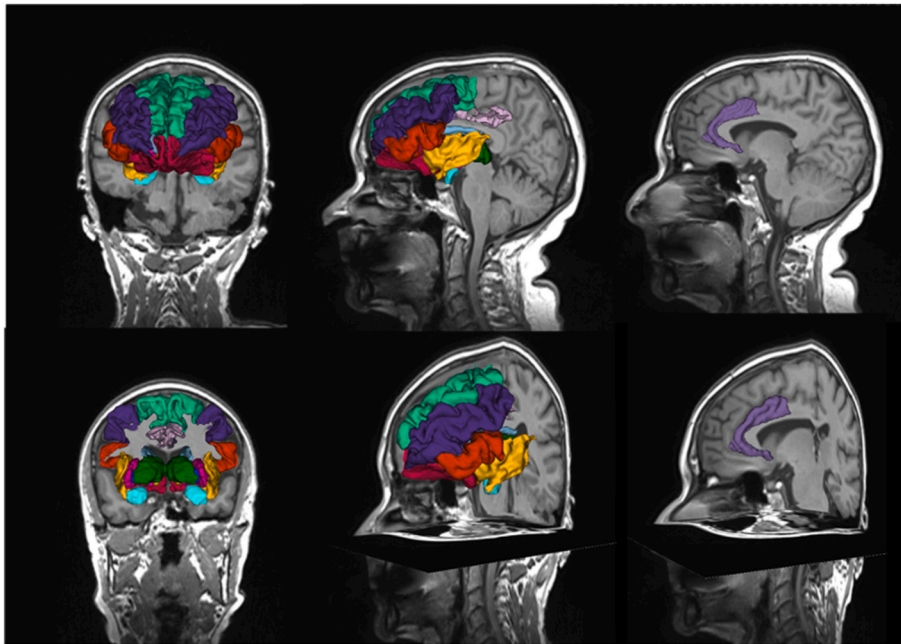


Fig. 5. CBF ROI-based analysis of apathy illustrated on one subject. First and second column: analyzed ROIs (dark green: thalamus, light blue: caudate, pink: putamen, dark blue: pallidum, yellow: insula, turquoise blue: amygdala, old pink: posterior cingulate, mauve: anterior cingulate gyrus, red: orbitofrontal cortex, orange: inferior frontal cortex, purple: middle frontal cortex, green: superior frontal cortex, dark yellow: accumbens. Third column: View of the left anterior cingulate gyrus.

apathy whereas increased nodal efficiency was for depression 1/apathy and depression has different cerebral patterns 2/salience-related processing in the ACC is related to apathy (Onoda and Yamaguchi, 2015). Our findings are consistent with these data in a sense that apathy in depression is characterized by a specific pathophysiological pattern. Ours brings additional evidence using another imaging modality, arterial spin labelling MRI. We think important to note that our result cannot be directly interpreted as a behavioral marker since our study was not designed for that purpose. A task-based imaging study, such as suggested by Cathomas and colleagues (Cathomas et al., 2015) would be a good complement to our study.

It could be interesting to separate the proper perfusion profile of dorsal versus subgenual ACC and its relationships with apathy intensity in our population of depressed patients. Indeed, dorsal ACC has been described with an integration role of reward/effort net value between the goal value (vmPFC) and effort cost (anterior insula) (Pessiglione et al., 2018). We could have hypothesized that in our study, higher levels of apathy in depressed patients would be associated with lower perfusion in more dorsal areas of ACC rather than ventral. As an exploratory step, we investigated this hypothesis to explore whether there is a difference in the effect between the rostral and caudal parts of the ACC. We performed the same stepwise regression analysis adding “ctx-caudal-anteriorcingulate” and “ctx-rostral-anteriorcingulate” ROIs from the Desikan-Killiany Atlas as two separate regressors. We found a significant relationship between AES and three ROIs:

- left caudal ACC (standardized beta = -0.50 , corrected p value = 0.0001)
- left OFC (standardized beta = -0.39 , corrected p value = 0.0028)
- right caudal ACC (standardized beta = 0.35 , corrected p value = 0.0182)

These results are in line with our findings as well as our hypothesis that higher levels of apathy in depressed patients would be associated with lower perfusion in more caudal areas of ACC rather than ventral. However, reliability metrics of our model showed that these results are less robust than the initial model. Indeed, the check for multicollinearity based on variance inflation factors (VIF) emphasized a lack of robustness

with too high VIF values (up to 8.69). Despite that this result would be an interesting addition, we believe that the model assessing caudal vs rostral ACC CBF is not robust enough to be considered as the main finding of our study. An independent study ran on another sample is needed to test and confirm this hypothesis.

4.3. The anterior cingulate cortex in depression and treatment response

As part of the mesolimbic dopaminergic pathway, ACC is known to be involved in the pathophysiology of depression specifically in relation to proactive and reactive behaviors (Post and Warden, 2018). It has been identified as a hub involved in reward related dimensions of depression (Cléry-Melin et al., 2019).

Neuroimaging studies have shown that apathy in depression has been linked with ACC structural abnormalities such as decrease of grey matter (Lavretsky et al., 2007), abnormal functional activity during effortful tasks (Elliott et al., 1997; Harvey et al., 2005; Pizzagalli et al., 2006).

Furthermore, decreased resting state functional connectivity (RSFC) between amygdala and dorsal ACC correlated to emotional processing deficit in adolescent depressed patients (Pannekoek et al., 2014). Thus, in elderly depression, decreased ACC – anterior insula RSFC has been proposed as a “biological” signature of late-life depression through the implication of salience network in motivation-related behaviors (Yuen et al., 2014). Taken together, ACC is a key region involved in the emotional and motivational processes guiding the regulation of pro vs. reactive behaviors. Our results are in line with these data and provide additional evidence supporting the implication of this structure to the motivational dimension of depression.

Finally, our study may open avenues on the therapeutic level. Indeed, ACC functional activity or connectivity has been widely reported as predictors of treatment response to several therapies: cognitive psychotherapy (Clark and Beck, 2010), antidepressant (Godlewska et al., 2018; Tian et al., 2020; Yuen et al., 2014a,b), repetitive transcranial magnetic stimulation (Downar and Daskalakis, 2013; Feffer et al., 2017; Ge et al., 2020). In addition, subgenual ACC is an historical target for deep brain stimulation in treatment resistant depression (Holtzheimer et al., 2017; Mayberg et al., 2005) with promising results.

By pinpointing a strong relationship between ACC and apathy in depressed patients, our study suggests that apathy could be considered as a relevant subtype in depression with a robust biological basis that could be explored as a potential therapeutic target in future works.

4.4. Hemispheric asymmetry of the ACC perfusion in relation to apathy

Hemispheric asymmetry has been reported in several perfusion studies on depression with increased perfusion in left cingulate cortex in adult (Kaichi et al., 2016) and remitted late onset depression (Liao et al., 2017) whereas the opposite direction has been described in a study on first episode mood depressive disorder (Chen et al., 2016). Some authors suggested that this hemispheric asymmetry may be mediated by the onset age and therapeutic status (Liao et al., 2017). Although functional and structural asymmetry has been reported in depression, the role of these hemispheric differences in its pathophysiology is still debated (Jiang et al., 2019).

In regards to goal-directed behaviors, interestingly, in line with our results, one study reported that action motivation (regardless of stimulus valence) was characterized by a greater fMRI activation in left (as compared to the right) dorsolateral prefrontal cortex in a task-based paradigm (Berkman and Lieberman, 2010). One study reported an opposite pattern of perfusion asymmetry in Alzheimer disease - as measured by single photon emission tomography - with a decreased perfusion in the right ACC associated with a lack of motivation (Benoit et al., 2004). This latter work reported findings in the opposite direction than ours. We must note that this study was conducted in a population of non-depressed patients.

Finally, we wanted to point out that the fact that the left and right ACC regression coefficients were in opposite directions - as opposed to initial correlation reported in the descriptive dendrogram - could be interpreted as a result of the strength of the negative relationship between AES and left ACC that is reported as the main finding.

4.5. Limitations

First, the inherently low spatial resolution of ASL did not allow a fine parcellation of the brain and the analysis of sub-regions of interest such striatum or pallidum. Second, the design of our study did not include any control group. A group of healthy subjects would have helped us to determine the baseline perfusion of the analyzed regions. Third, we have to mention the cross-sectional design of our study. Indeed, we did not investigate the predictive value of CBF in the clinical context of depression but rather focused on understanding the neurobiological underpinnings of apathy in adult depression by assessing the relationship between CBF and apathy in a cross-sectional design. Note that we are currently conducting a longitudinal study with two imaging time-points to identify biomarkers predictive of the negative course of the depressive illness (<https://clinicaltrials.gov/ct2/show/study/NCT03690856>). Fourth, given our specific a priori hypotheses based on foundational works from Berridge and Robinson, and Le Heron (Berridge et al., 2009; Le Heron et al., 2019), we conducted an ROI rather than a whole brain analysis. A whole-brain analysis could bring additional insight on the neurobiological basis of apathy in depression. Fifth, we used a stepwise regression model to test our hypothesis which can be discussed considering the alternative use of a standard multiple regression model without variable selection. This choice was driven by using a competitive model along a stepwise fitting method that seems better suited to account for the complexity of brain pathophysiology and deal with inter-region brain perfusion correlation (as highlighted by our dendrogram analysis). Furthermore, we have provided provided the additional validation metrics of the final model and variable inclusion procedure in the supplementary material. Further studies are necessary to overcome these limitations.

5. Conclusion

This study focused on perfusion patterns of apathetic dimension in depressed patients. Our results highlight that apathy was specifically associated with brain perfusion patterns. Interestingly, we have shown that some perfusion patterns underline the clinical specificities of apathy in depression (Batail et al., 2018). Furthermore, these abnormalities affect key regions involved in the meso-cortico-limbic dopaminergic loop of the reward system. The most striking result was a strong negative relationship between the CBF in the left ACC and the AES score. Therefore, apathy appears to be a relevant marker to better characterize different phenotypes of depression. Identifying the radiological and clinical specificities of apathy in depression would provide a better understanding of its underlying neurobiological mechanisms and would help to better adjust treatment. Our work brings a better understanding of the pathophysiology of apathy in depression and therefore may inform the development of some specific treatment for this particular subtype such as dopaminergic targeted pharmacologic strategies, pramipexole (Cusin et al., 2013) or new cerebral targets for non-pharmacological treatments like repetitive transcranial magnetic stimulation of dorso-medial prefrontal cortex (Downar and Daskalakis, 2013; Feffer et al., 2017) or neurofeedback (Arns et al., 2017).

Declaration of competing interest

The authors don't have any conflict of interest related to this research work.

Acknowledgments

MRI data acquisition was supported by the Neurinfo MRI research facility from the University of Rennes I. Neurinfo is granted by the European Union (FEDER), the French State, the Brittany Council, Rennes Metropole, Inria, Inserm and the University Hospital of Rennes. This work has been funded by Institut des Neurosciences Cliniques de Rennes (INCR). The authors thank Mr Stéphane Brousse and Mr Jacques Soulabaille for their involvement in the conduct of the study.

Appendix A. Supplementary data

Supplementary data to this article can be found online at <https://doi.org/10.1016/j.jpsychires.2022.11.015>.

References

- Alexopoulos, G.S., Hoptman, M.J., Yuen, G., Kanellopoulos, D., Seirup, K., J. Lim, K.O., Gunning, F.M., 2012. Functional connectivity in apathy of late-life depression: a preliminary study. *Journal of Affective Disorders*. <https://doi.org/10.1016/j.jad.2012.11.023>.
- Almeida, J.R.C., Akkal, D., Hassel, S., Travis, M.J., Banihashemi, L., Kerr, N., Kupfer, D. J., Phillips, M.L., 2009. Reduced gray matter volume in ventral prefrontal cortex but not amygdala in bipolar disorder: significant effects of gender and trait anxiety. *Psychiatr. Res. Neuroimaging* 171 (1), 54–68. <https://doi.org/10.1016/j.psychres.2008.02.001>.
- Alsop, D.C., Detre, J.A., Golay, X., Günther, M., Hendrikse, J., Hernandez-Garcia, L., Lu, H., MacIntosh, B.J., Parkes, L.M., Smits, M., van Osch, M.J.P., Wang, D.J.J., Wong, E.C., Zaharchuk, G., 2015. Recommended implementation of arterial spin-labeled perfusion MRI for clinical applications: a consensus of the ISMRM perfusion study group and the European consortium for ASL in dementia: recommended Implementation of ASL for Clinical Applications. *Magn. Reson. Med.* 73 (1), 102–116. <https://doi.org/10.1002/mrm.25197>.
- Arnold, B.A., Blasey, C., Williams, L.M., Palmer, D.M., Rekshan, W., Schatzberg, A.F., Etkin, A., Kulkarni, J., Luther, J.F., Rush, A.J., 2015. Depression subtypes in predicting antidepressant response: a report from the iSPOT-D trial. *Am. J. Psychiatr.* 172 (8), 743–750. <https://doi.org/10.1176/appi.ajp.2015.14020181>.
- Arns, M., Batail, J.-M., Bioulac, S., Congedo, M., Daudet, C., Drapier, D., Fovet, T., Jardri, R., Le-Van-Quyen, M., Lotte, F., Mehler, D., Micoulaud-Franchi, J.-A., Purper-Ouakil, D., Vialatte, F., 2017. Neurofeedback: one of today's techniques in psychiatry? *L'Encéphale* 43 (2), 135–145. <https://doi.org/10.1016/j.encep.2016.11.003>.

- Arns, M., van Dijk, H., Luyck, J.J., van Wingen, G., Olbrich, S., 2022. Stratified psychiatry: tomorrow's precision psychiatry? *Eur. Neuropsychopharmacol.* 55, 14–19. <https://doi.org/10.1016/j.euroneuro.2021.10.863>.
- Ashburner, J., Friston, K.J., 2005. Unified segmentation. *Neuroimage* 26 (3), 839–851. <https://doi.org/10.1016/j.neuroimage.2005.02.018>.
- Baggio, H.C., Segura, B., Garrido-Millan, J.L., Marti, M.-J., Compta, Y., Valldeoriola, F., Tolosa, E., Junque, C., 2015. Resting-state frontostriatal functional connectivity in Parkinson's disease-related apathy: frontostriatal connectivity and apathy in pd. *Mov. Disord.* 30 (5), 671–679. <https://doi.org/10.1002/mds.26137>.
- Barillot, C., Bannier, E., Commowick, O., Corouge, I., Baire, A., Fakhfakh, I., Guillaumont, J., Yao, Y., Kain, M., 2016. Shanoir: applying the software as a service distribution model to manage brain imaging research repositories. *Frontiers in ICT* 3. <https://doi.org/10.3389/fict.2016.00025>.
- Batail, J.M., Palaric, J., Guillery, M., Gadoullet, J., Sauleau, P., Le Jeune, F., Vérin, M., Robert, G., Drapier, D., 2018. Apathy and depression: which clinical specificities? *Personalized Medicine in Psychiatry* 7–8, 21–26. <https://doi.org/10.1016/j.pmp.2017.12.001>.
- Benoit, M., Clairet, S., Koulibaly, P.M., Darcourt, J., Robert, P.H., 2004. Brain perfusion correlates of the apathy inventory dimensions of Alzheimer's disease. *Int. J. Geriatr. Psychiatr.* 19 (9), 864–869. <https://doi.org/10.1002/gps.1163>.
- Benoit, M., Robert, P.H., 2011. Imaging correlates of apathy and depression in Parkinson's disease. *J. Neurol. Sci.* 310 (1–2), 58–60. <https://doi.org/10.1016/j.jns.2011.07.006>.
- Berkman, E.T., Lieberman, M.D., 2010. Approaching the bad and avoiding the good: lateral prefrontal cortical asymmetry distinguishes between action and valence. *J. Cognit. Neurosci.* 22 (9), 1970–1979. <https://doi.org/10.1162/jocn.2009.21317>.
- Berridge, K., Robinson, T., Aldridge, J., 2009. Dissecting components of reward: 'Liking', 'wanting', and learning. *Curr. Opin. Pharmacol.* 9 (1), 65–73. <https://doi.org/10.1016/j.coph.2008.12.014>.
- Bonnelle, V., Manohar, S., Behrens, T., Husain, M., 2016. Individual differences in premotor brain systems underlie behavioral apathy. *Cerebral Cortex* (New York, N. Y.: 1991) 26 (2), 807–819. <https://doi.org/10.1093/cercor/bhv247>.
- Braem, S., King, J.A., Korb, F.M., Krebs, R.M., Notebaert, W., Egner, T., 2017. The role of the anterior cingulate cortex in the affective evaluation of conflict. *J. Cognit. Neurosci.* 29 (1), 137–149. https://doi.org/10.1162/jocn_a.01023.
- Brockett, A.T., Tennyson, S.S., deBettencourt, C.A., Gaye, F., Roesch, M.R., 2020. Anterior cingulate cortex is necessary for adaptation of action plans. *Proc. Natl. Acad. Sci. U. S. A.* 117 (11), 6196–6204. <https://doi.org/10.1073/pnas.1919303117>.
- Buxton, R.B., Frank, L.R., Wong, E.C., Siewert, B., Warach, S., Edelman, R.R., 1998. A general kinetic model for quantitative perfusion imaging with arterial spin labeling. *Magn. Reson. Med.* 40 (3), 383–396.
- Cathomas, F., Hartmann, M.N., Seifritz, E., Pryce, C.R., Kaiser, S., 2015. The translational study of apathy—an ecological approach. *Front. Behav. Neurosci.* 9 <https://doi.org/10.3389/fnbeh.2015.00241>.
- Chen, G., Bian, H., Jiang, D., Cui, M., Ji, S., Liu, M., Lang, X., Zhuo, C., 2016. Pseudo-continuous arterial spin labeling imaging of cerebral blood perfusion asymmetry in drug-naïve patients with first-episode major depression. *Biomedical Reports* 5 (6), 675–680. <https://doi.org/10.3892/br.2016.796>.
- Chen, A.C., Oathes, D.J., Chang, C., Bradley, T., Zhou, Z.-W., Williams, L.M., Glover, G.H., Deisseroth, K., Etkin, A., 2013. Causal interactions between fronto-parietal central executive and default-mode networks in humans. *Proc. Natl. Acad. Sci. U. S. A.* 110 (49), 19944–19949. <https://doi.org/10.1073/pnas.1311772110>.
- Clark, D.A., Beck, A.T., 2010. Cognitive theory and therapy of anxiety and depression: convergence with neurobiological findings. *Trends Cognit. Sci.* 14 (9), 418–424. <https://doi.org/10.1016/j.tics.2010.06.007>.
- Cléry-Melin, M.-L., Jollant, F., Gorwood, P., 2019. Reward systems and cognitions in major depressive disorder. *CNS Spectr.* 24 (1), 64–77. <https://doi.org/10.1017/S1092852918001335>.
- Colloby, S.J., Firkbank, M.J., He, J., Thomas, A.J., Vasudev, A., Parry, S.W., O'Brien, J.T., 2012. Regional cerebral blood flow in late-life depression: arterial spin labelling magnetic resonance study. *The British Journal of Psychiatry: J. Ment. Sci.* 200 (2), 150–155. <https://doi.org/10.1192/bjp.bp.111.092387>.
- Cusin, C., Iovieno, N., Iosifescu, D.V., Nierenberg, A.A., Fava, M., Rush, A.J., Perlis, R.H., 2013. A randomized, double-blind, placebo-controlled trial of pramipexole augmentation in treatment-resistant major depressive disorder. *J. Clin. Psychiatr.* 74 (7), e636–e641. <https://doi.org/10.4088/JCP.12m08093>.
- Desikan, R.S., Segonne, F., Fischl, B., Quinn, B.T., Dickerson, B.C., Blacker, D., Buckner, R.L., Dale, A.M., Maguire, R.P., Hyman, B.T., Albert, M.S., Killiany, R.J., 2006. An automated labeling system for subdividing the human cerebral cortex on MRI scans into gyral based regions of interest. *Neuroimage* 31 (3), 968–980.
- Detre, J.A., Leigh, J.S., Williams, D.S., Koretsky, A.P., 1992. Perfusion imaging. *Magnetic Resonance in Medicine: Official Journal of the Society of Magnetic Resonance in Medicine / Society of Magnetic Resonance in Medicine* 23 (1), 37–45.
- Detre, John A., Rao, H., Wang, D.J.J., Chen, Y.F., Wang, Z., 2012. Applications of arterial spin labeled MRI in the brain. *J. Magn. Reson. Imag.* 35 (5), 1026–1037. <https://doi.org/10.1002/jmri.23581>.
- Devinsky, O., Morrell, M.J., Vogt, B.A., 1995. Contributions of anterior cingulate cortex to behaviour. *Brain: J. Neurol.* 118 (Pt 1), 279–306. <https://doi.org/10.1093/brain/118.1.279>.
- Downar, J., Daskalakis, Z.J., 2013. New targets for rTMS in depression: a review of convergent evidence. *Brain Stimul.* 6 (3), 231–240. <https://doi.org/10.1016/j.brs.2012.08.006>.
- Duhameau, B., Ferré, J.-C., Jannin, P., Gauvrit, J.-Y., Vérin, M., Millet, B., Drapier, D., 2010. Chronic and treatment-resistant depression: a study using arterial spin labeling perfusion MRI at 3Tesla. *Psychiatry Research: Neuroimaging* 182 (2), 111–116. <https://doi.org/10.1016/j.pscychresns.2010.01.009>.
- Elliott, R., Sahakian, B.J., Herrod, J.J., Robbins, T.W., Paykel, E.S., 1997. Abnormal response to negative feedback in unipolar depression: evidence for a diagnosis specific impairment. *J. Neurol. Neurosurg. Psychiatr.* 63 (1), 74–82. <https://doi.org/10.1136/jnnp.63.1.74>.
- Etkin, A., Büchel, C., Gross, J.J., 2015. The neural bases of emotion regulation. *Nature Reviews Neuroscience* 16 (11), 693–700. <https://doi.org/10.1038/nrn4044>.
- Feffer, K., Peters, S.K., Bhui, K., Downar, J., Giacobbe, P., 2017. Successful dorsomedial prefrontal rTMS for major depression in borderline personality disorder: three cases. *Brain Stimul.* 10 (3), 716–717. <https://doi.org/10.1016/j.brs.2017.01.583>.
- Ferré, J.-C., Bannier, E., Raoult, H., Mineur, G., Carsin-Nicol, B., Gauvrit, J.-Y., 2013. Arterial spin labeling (ASL) perfusion: techniques and clinical use. *Diagnostic and Interventional Imaging.* <https://doi.org/10.1016/j.diii.2013.06.010>.
- Freels, S., Cohen, D., Eisdorfer, C., Paveza, G., Gorelick, P., Luchins, D.J., Hirschman, R., Ashford, J.W., Levy, P., Semla, T., 1992. Functional status and clinical findings in patients with Alzheimer's disease. *J. Gerontol.* 47 (6), M177–M182. <https://doi.org/10.1093/geronj/47.6.m177>.
- Gaillard, R., Gourion, D., Llorca, P.M., 2013. [Anhedonia in depression]. *L'Encéphale* 39 (4), 296–305. <https://doi.org/10.1016/j.encep.2013.07.001>.
- Gasquoine, P.G., 2013. Localization of function in anterior cingulate cortex: from psychosurgery to functional neuroimaging. *Neurosci. Biobehav. Rev.* 37 (3), 340–348. <https://doi.org/10.1016/j.neubiorev.2013.01.002>.
- Ge, R., Downar, J., Blumberger, D.M., Daskalakis, Z.J., Vila-Rodriguez, F., 2020. Functional connectivity of the anterior cingulate cortex predicts treatment outcome for rTMS in treatment-resistant depression at 3-month follow-up. *Brain Stimul.* 13 (1), 206–214. <https://doi.org/10.1016/j.brs.2019.10.012>.
- Godlewski, B.R., Browning, M., Norbury, R., Igoumenou, A., Cowen, P.J., Harmer, C.J., 2018. Predicting treatment response in depression: the role of anterior cingulate cortex. *Int. J. Neuropsychopharmacol.* 21 (11), 988–996. <https://doi.org/10.1093/ijnp/pyy069>.
- Haller, S., Zaharchuk, G., Thomas, D.L., Lovblad, K.-O., Barkhof, F., Golay, X., 2016. Arterial spin labeling perfusion of the brain: emerging clinical applications. *Radiology* 281 (2), 337–356. <https://doi.org/10.1148/radiol.2016150789>.
- Harvey, P.-O., Fossati, P., Pochon, J.-B., Levy, R., LeBastard, G., LeHéricy, S., Allilaire, J.-F., Dubois, B., 2005. Cognitive control and brain resources in major depression: an fMRI study using the n-back task. *Neuroimage* 26 (3), 860–869.
- Hillary, F.G., Roman, C.A., Venkatesan, U., Rajtmajer, S.M., Bajo, R., Castellanos, N.D., 2015. Hyperconnectivity is a fundamental response to neurological disruption. *Neuropsychology* 29 (1), 59–75. <https://doi.org/10.1037/neu0000110>.
- Ho, T.C., Wu, J., Shin, D.D., Liu, T.T., Tapert, S.F., Yang, G., Connolly, C.G., Frank, G.K.W., Max, J.E., Wolkowitz, O., Eisendrath, S., Hoefl, F., Banerjee, D., Hood, K., Hendren, R.L., Paulus, M.P., Simmons, A.N., Yang, T.T., 2013. Altered cerebral perfusion in executive, affective, and motor networks during adolescent depression. *J. Am. Acad. Child Adolesc. Psychiatry* 52 (10), 1076–1091. <https://doi.org/10.1016/j.jaac.2013.07.008>.
- Holroyd, C.B., McClure, S.M., 2015. Hierarchical control over effortful behavior by rodent medial frontal cortex: a computational model. *Psychol. Rev.* 122 (1), 54–83. <https://doi.org/10.1037/a0038339>.
- Holroyd, C.B., Yeung, N., 2012. Motivation of extended behaviors by anterior cingulate cortex. *Trends Cognit. Sci.* 16 (2), 122–128. <https://doi.org/10.1016/j.tics.2011.12.008>.
- Holtzheimer, P.E., Husain, M.M., Lisanby, S.H., Taylor, S.F., Whitworth, L.A., McClintock, S., Slavin, K.V., Berman, J., McKhann, G.M., Patil, P.G., Rittberg, B.R., Abosch, A., Pandurangi, A.K., Holloway, K.L., Lam, R.W., Honey, C.R., Neimat, J.S., Hendershot, J.M., DeBattista, C., et al., 2017. Subcallosal cingulate deep brain stimulation for treatment-resistant depression: a multisite, randomised, sham-controlled trial. *Lancet Psychiatr.* 4 (11), 839–849. [https://doi.org/10.1016/S2215-0366\(17\)30371-1](https://doi.org/10.1016/S2215-0366(17)30371-1).
- Iglewicz, B., Hoaglin, D.C., 1993. *How to Detect and Handle Outliers*, vol. 16. *Asq Press*.
- Jiang, X., Shen, Y., Yao, J., Zhang, L., Xu, L., Feng, R., Cai, L., Liu, J., Chen, W., Wang, J., 2019. Connectome analysis of functional and structural hemispheric brain networks in major depressive disorder. *Transl. Psychiatry* 9 (1), 1–12. <https://doi.org/10.1038/s41398-019-0467-9>.
- Kaichi, Y., Okada, G., Takamura, M., Toki, S., Akiyama, Y., Higaki, T., Matsubara, Y., Okamoto, Y., Yamawaki, S., Awai, K., 2016. Changes in the regional cerebral blood flow detected by arterial spin labeling after 6-week escitalopram treatment for major depressive disorder. *J. Affect. Disord.* 194, 135–143. <https://doi.org/10.1016/j.jad.2015.12.062>.
- Kang, J.Y., Lee, J.S., Kang, H., Lee, H.-W., Kim, Y.K., Jeon, H.J., Chung, J.-K., Lee, M.C., Cho, M.J., Lee, D.S., 2012. Regional cerebral blood flow abnormalities associated with apathy and depression in alzheimer disease. *Alzheimer Dis. Assoc. Disord.* 26 (3), 217–224. <https://doi.org/10.1097/WAD.0b013e318231e5fc>.
- Kolling, N., Wittmann, M., Behrens, T., Boorman, E., Mars, R., Rushworth, M., 2016. Anterior cingulate cortex and the value of the environment, search, persistence, and model updating. *Nat. Neurosci.* 19 (10), 1280–1285. <https://doi.org/10.1038/nn.4382>.
- Kos, C., van Tol, M.-J., Marsman, J.-B.C., Knegeter, H., Aleman, A., 2016. Neural correlates of apathy in patients with neurodegenerative disorders, acquired brain injury, and psychiatric disorders. *Neurosci. Biobehav. Rev.* 69, 381–401. <https://doi.org/10.1016/j.neubiorev.2016.08.012>.
- Kostić, V.S., Filippi, M., 2011. Neuroanatomical correlates of depression and apathy in Parkinson's disease: magnetic resonance imaging studies. *J. Neurol. Sci.* 310 (1–2), 61–63. <https://doi.org/10.1016/j.jns.2011.05.036>.
- Lavretsky, H., Ballmaier, M., Pham, D., Toga, A., Kumar, A., 2007. Neuroanatomical characteristics of geriatric apathy and depression: a magnetic resonance imaging

- study. *Am. J. Geriatr. Psychiatr.* 15 (5), 386–394. <https://doi.org/10.1097/JGP.0b013e3180325a16>.
- Lavin, C., Melis, C., Mikulan, E., Gelormini, C., Huepe, D., Ibanez, A., 2013. The anterior cingulate cortex: an integrative hub for human socially-driven interactions. *Front. Neurosci.* 7. <https://www.frontiersin.org/article/10.3389/fnins.2013.00064>.
- Le Heron, C., Holroyd, C.B., Salamone, J., Husain, M., 2019. Brain mechanisms underlying apathy. *J. Neurol. Neurosurg. Psychiatr.* 90 (3), 302–312. <https://doi.org/10.1136/jnnp-2018-318265>.
- Liao, W., Wang, Z., Zhang, X., Shu, H., Wang, Z., Liu, D., Zhang, Z., 2017. Cerebral blood flow changes in remitted early- and late-onset depression patients. *Oncotarget* 8 (44), 76214–76222. <https://doi.org/10.18632/oncotarget.19185>.
- Lui, S., Parkes, L.M., Huang, X., Zou, K., Chan, R.C., Yang, H., Zou, L., Li, D., Tang, H., Zhang, T., 2009. Depressive disorders: focally altered cerebral perfusion measured with arterial spin-labeling MR imaging. *Radiology* 251 (2), 476–484.
- Marin, null, 1996. Apathy: concept, syndrome, neural mechanisms, and treatment. *Semin. Clin. Neuropsychiatry* 1 (4), 304–314. <https://doi.org/10.1053/SCNP00100304>.
- Marin, R.S., 1990. Differential diagnosis and classification of apathy. *Am. J. Psychiatr.* 147 (1), 22–30. <https://doi.org/10.1176/ajp.147.1.22>.
- Marin, R.S., 1991. Apathy: a neuropsychiatric syndrome. *J. Neuropsychiatry Clin. Neurosci.* 3 (3), 243–254. <https://doi.org/10.1176/jnp.3.3.243>.
- Maumet, C., Maurel, P., Ferré, J.-C., Barillot, C., 2014. Robust estimation of the cerebral blood flow in arterial spin labelling. *Magn. Reson. Imag.* 32 (5), 497–504. <https://doi.org/10.1016/j.mri.2014.01.016>.
- Mayberg, H.S., Lozano, A.M., Voon, V., McNeely, H.E., Seminowicz, D., Hamani, C., Schwab, J.M., Kennedy, S.H., 2005. Deep brain stimulation for treatment-resistant depression. *Neuron* 45 (5), 651–660. <https://doi.org/10.1016/j.neuron.2005.02.014>.
- Montgomery, S.A., Asberg, M., 1979. A new depression scale designed to be sensitive to change. *Br. J. Psychiatr.: J. Ment. Sci.* 134, 382–389.
- Onoda, K., Yamaguchi, S., 2015. Dissociative contributions of the anterior cingulate cortex to apathy and depression: topological evidence from resting-state functional MRI. *Neuropsychologia* 77, 10–18. <https://doi.org/10.1016/j.neuropsychologia.2015.07.030>.
- Orosz, A., Jann, K., Federspiel, A., Horn, H., Höfle, O., Dierks, T., Wiest, R., Strik, W., Müller, T., Walther, S., 2012. Reduced cerebral blood flow within the default-mode network and within total gray matter in major depression. *Brain Connect.* 2 (6), 303–310. <https://doi.org/10.1089/brain.2012.0101>.
- Pannekoek, J.N., van der Werff, S.J.A., Meens, P.H.F., van den Bulk, B.G., Jolles, D.D., Veer, I.M., van Lang, N.D.J., Rombouts, S.A.R.B., van der Wee, N.J.A., Vermeiren, R. R.J.M., 2014. Aberrant resting-state functional connectivity in limbic and salience networks in treatment-naïve clinically depressed adolescents. *J. Child Psychol. Psychiatry Allied Discip.* 55 (12), 1317–1327. <https://doi.org/10.1111/jcpp.12266>.
- Pessiglione, M., Vinckier, F., Bouret, S., Daunizeau, J., Le Bouc, R., 2018. Why not try harder? Computational approach to motivation deficits in neuro-psychiatric diseases. *Brain* 141 (3), 629–650. <https://doi.org/10.1093/brain/awx278>.
- Petersen, E.T., Mouridsen, K., Golay, X., 2010. The QUASAR reproducibility study, Part II: results from a multi-center Arterial Spin Labeling test-retest study. *Neuroimage* 49 (1), 104–113. <https://doi.org/10.1016/j.neuroimage.2009.07.068> all named co-authors of the QUASAR test-retest study.
- Pizzagalli, D.A., Peccoralo, L.A., Davidson, R.J., Cohen, J.D., 2006. Resting anterior cingulate activity and abnormal responses to errors in subjects with elevated depressive symptoms: a 128-channel EEG study. *Hum. Brain Mapp.* 27 (3), 185–201. <https://doi.org/10.1002/hbm.20172>.
- Post, R.J., Warden, M.R., 2018. Melancholy, anhedonia, apathy: the search for separable behaviors and neural circuits in depression. *Curr. Opin. Neurobiol.* 49, 192–200. <https://doi.org/10.1016/j.conb.2018.02.018>.
- Prakash, K.M., Nadkarni, N.V., Lye, W.-K., Yong, M.-H., Tan, E.-K., 2016. The impact of non-motor symptoms on the quality of life of Parkinson's disease patients: a longitudinal study. *Eur. J. Neurol.* 23 (5), 854–860. <https://doi.org/10.1111/ene.12950>.
- Robert, G., Le Jeune, F., Dondaine, T., Drapier, S., Peron, J., Lozachmeur, C., Sauleau, P., Houvenaghel, J.-F., Travers, D., Millet, B., Verin, M., Drapier, D., 2014. Apathy and impaired emotional facial recognition networks overlap in Parkinson's disease: a PET study with conjunction analyses. *J. Neurol. Neurosurg. Psychiatr.* 85 (10), 1153–1158. <https://doi.org/10.1136/jnnp-2013-307025>.
- Robert, Gabriel, Bannier, E., Comte, M., Domain, L., Corouge, I., Dondaine, T., Batail, J.-M., Ferre, J.-C., Fakra, E., Drapier, D., 2021. Multimodal brain imaging connectivity analyses of emotional and motivational deficits in depression among women. *J. Psychiatry Neurosci.: JPN* 46 (2), E303–E312. <https://doi.org/10.1503/jpn.200074>.
- Robert, Gabriel, Le Jeune, F., Lozachmeur, C., Drapier, S., Dondaine, T., Péron, J., Travers, D., Sauleau, P., Millet, B., Verin, M., 2012. Apathy in patients with Parkinson disease without dementia or depression A PET study. *Neurology* 79 (11), 1155–1160.
- Sheehan, D.V., Lecrubier, Y., Sheehan, K.H., Amorim, P., Janavs, J., Weiller, E., Hergueta, T., Baker, R., Dunbar, G.C., 1998. The Mini-International Neuropsychiatric Interview (M.I.N.I.): the development and validation of a structured diagnostic psychiatric interview for DSM-IV and ICD-10. *J. Clin. Psychiatr.* 59 (Suppl. 20), 22–33 quiz 34–57.
- Snaith, R.P., Hamilton, M., Morley, S., Humayan, A., Hargreaves, D., Trigwell, P., 1995. A scale for the assessment of hedonic tone the Snaith-Hamilton Pleasure Scale. *Br. J. Psychiatr.* 167 (1), 99–103. <https://doi.org/10.1192/bjp.167.1.99>.
- Spielberger, C.D., Gorsuch, R.L., Lushene, R.E., 1970. *Manual for the State-Trait Anxiety Inventory*.
- Stevens, F.L., Hurley, R.A., Taber, K.H., Hurley, R.A., Hayman, L.A., Taber, K.H., 2011. Anterior cingulate cortex: unique role in cognition and emotion. *J. Neuropsychiatry Clin. Neurosci.* 23 (2), 121–125. <https://doi.org/10.1176/jnp.23.2.jnp121>.
- Théberge, J., 2008. Perfusion magnetic resonance imaging in psychiatry. *Top. Magn. Reson. Imag.* 19 (2), 111–130. <https://doi.org/10.1097/RMR.0b013e3181808140>.
- Thelertis, C., Politis, A., Siarkos, K., Lyketsos, C.G., 2014. A review of neuroimaging findings of apathy in Alzheimer's disease. *Int. Psychogeriatr.* 26 (2), 195–207. <https://doi.org/10.1017/S1041610213001725>.
- Tian, S., Sun, Y., Shao, J., Zhang, S., Mo, Z., Liu, X., Wang, Q., Wang, L., Zhao, P., Chattun, M.R., Yao, Z., Si, T., Lu, Q., 2020. Predicting escitalopram monotherapy response in depression: the role of anterior cingulate cortex. *Hum. Brain Mapp.* 41 (5), 1249–1260. <https://doi.org/10.1002/hbm.24872>.
- Treadway, M.T., Zald, D.H., 2011. Reconsidering anhedonia in depression: lessons from translational neuroscience. *Neurosci. Biobehav. Rev.* 35 (3), 537–555. <https://doi.org/10.1016/j.neubiorev.2010.06.006>.
- van Reekum, R., Stuss, D.T., Ostrander, L., 2005. Apathy: why care? The journal of neuropsychiatry and clinical Neuroscience. <http://neuro.psychiatryonline.org/doi/pdf/10.1176/jnp.17.1.7>.
- Vicini Chilovi, B., Conti, M., Zanetti, M., Mazzù, I., Rozzini, L., Padovani, A., 2009. Differential impact of apathy and depression in the development of dementia in mild cognitive impairment patients. *Dement. Geriatr. Cognit. Disord.* 27 (4), 390–398. <https://doi.org/10.1159/000210045>.
- Watts, J.M., Whitlow, C.T., Maldjian, J.A., 2013. Clinical applications of arterial spin labeling: clinical applications of MR arterial spin-labeled perfusion imaging. *NMR Biomed.* 26 (8), 892–900. <https://doi.org/10.1002/nbm.2904>.
- Wen, M.C., Chan, L.L., Tan, L.C.S., Tan, E.K., 2016. Depression, anxiety, and apathy in Parkinson's disease: insights from neuroimaging studies. *Eur. J. Neurol.* 23 (6), 1001–1019. <https://doi.org/10.1111/ene.13002>.
- Widlöcher, D.J., 1983. Psychomotor retardation: clinical, theoretical, and psychometric aspects. *Psychiatr. Clin.* 6 (1), 27–40.
- Wolf, R.L., Detre, J.A., 2007. Clinical neuroimaging using arterial spin-labeled perfusion magnetic resonance imaging. *Neurotherapeutics* 4 (3), 346–359. <https://doi.org/10.1016/j.nurt.2007.04.005>.
- Wu, W.-C., Fernández-Seara, M., Detre, J.A., Wehrli, F.W., Wang, J., 2007. A theoretical and experimental investigation of the tagging efficiency of pseudocontinuous arterial spin labeling. *Magn. Reson. Med.* 58 (5), 1020–1027. <https://doi.org/10.1002/mrm.21403>.
- Yuen, G.S., Gunning, F.M., Woods, E., Klimstra, S.A., Hoptman, M.J., Alexopoulos, G.S., 2014a. Neuroanatomical correlates of apathy in late-life depression and antidepressant treatment response. *J. Affect. Disord.* 166, 179–186. <https://doi.org/10.1016/j.jad.2014.05.008>.
- Yuen, G.S., Gunning-Dixon, F.M., Hoptman, M.J., AbdelMalak, B., McGovern, A.R., Seirup, J.K., Alexopoulos, G.S., 2014b. The salience network in the apathy of late-life depression: salience network in apathy of late-life depression. *Int. J. Geriatr. Psychiatr.* 29 (11), 1116–1124. <https://doi.org/10.1002/gps.4171>.
- Zahodne, L.B., Tremont, G., 2013. Unique effects of apathy and depression signs on cognition and function in amnesic mild cognitive impairment: apathy and depression in mild cognitive impairment. *Int. J. Geriatr. Psychiatr.* 28 (1), 50–56. <https://doi.org/10.1002/gps.3789>.